Med Bio Eng Comput (2007) 45:447–457
DOI 10.1007/s11517-007-0168-z

ORIGINAL ARTICLE

Electro-mechanical stability of surface EMG sensors

S. H. Roy · G. De Luca · M. S. Cheng · A. Johansson · L. D. Gilmore · C. J. De Luca

Received: 2 June 2006 / Accepted: 11 January 2007 / Published online: 16 February 2007

Abstract This study compared the performance of surface electromyographic (sEMG) sensors for different detection conditions affecting the electro-mechanical stability between the sensor and its contact with the skin. These comparisons were made to gain a better understanding of how specific characteristics of sensor design and use may alter the ability of sEMG sensors to detect signals with high fidelity under conditions of vigorous activity. The first part of the study investigated the effect of different detection surface contours and adhesive tapes on the ability of the sensor to remain in electrical contact with the skin. The second part of the study investigated the effects of different skin preparations and hydrophilic gels on the production of movement artifact resulting from sinusoidal and impact mechanical perturbations. Both parts of the study evaluated sensor performance under dry skin and wet skin (from perspiration) conditions. We found that contouring the detection surface and adding a more adhesive double-sided tape were effective in increasing the forces needed to disrupt the electrical contact between the electrodes and the skin for both dry skin and wet skin conditions. The mechanical perturbation tests demonstrated that hydrophilic gel applied to the detection surface of the sensor produced greater movement artifacts compared to sensors without gel, particularly when the sensors were tested under conditions in which perspiration was present on the skin. The use of a surfactant skin preparation did not influence the amount of movement artifacts that resulted from either the sinusoidal or impact perturbations. The importance of these findings is discussed in terms of their implications for improving sEMG signal fidelity through sensor design modifications and procedures for interfacing them with the skin.

Keywords Electromyography · Motion artifact · Sensor · EMG · Electrode · Peel force

S. H. Roy (✉) · L. D. Gilmore · C. J. De Luca
NeuroMuscular Research Center, Boston University,
19 Deerfield Street, 4th Floor, Boston, MA 02215, USA
e-mail: sroy@bu.edu

G. De Luca · M. S. Cheng · A. Johansson ·
C. J. De Luca
Delsys, Inc., Boston, MA 02215, USA

1 Introduction

Since their introduction by Piper [18], sensors for detecting the surface electromyographic (sEMG) signal have been widely used by researchers and clinicians interested in measuring the electrical signal that emanates from contracting muscles. The usefulness of the sEMG signal for measuring human performance was demonstrated by Inman [14] when he investigated the technical aspects of human locomotion. By the early 1960s, improvements in signal quality and convenience made sEMG sensors a common tool in clinical and research laboratories. Despite their popularity, current recording methods can be problematic in maintaining signal fidelity when vigorous or long-duration activities are monitored [22].

The sEMG sensor is an electrochemical transducer that detects biopotentials using metallic contacts placed on the skin tissue. The transducing element depends on the ability of the interface between the sensor and skin to conduct an exchange between the ionic current of the various tissue media and the

electron current flow of the recording instrumentation [9]. The ideal sensor would enable this exchange to occur with equal ease in either direction without forming a charge build-up or gradient at the interface [1, 3]. Unwanted contamination of the EMG signal by predominantly stochastic noise occurs when the flow of ions between the electrode–skin interface changes, producing variable net potential differences for pairs of electrodes placed on the skin [10]. Changes in the physical properties of the skin, such as an increase in moisture from perspiration, can compound such sources of noise. Other more deterministic contaminants may be present from power-line interference or movement of sensor leads [17].

Surface EMG sensors are currently available in a variety of detection geometries and encapsulations that can be interfaced with the skin using conductive hydrophilic gels, pastes, or wetting agents in conjunction with single- or double-sided adhesive tapes. Comparative studies of the electro-mechanical performance of commercially available sEMG sensors and the methods used to interface them with the skin are extremely limited in the literature. A few studies can be found which describe the effects of skin abrasion [21] and the use of conductive gels [23] on reducing skin impedance and motion artifact. Other studies have compared baseline electric noise and offset potentials for dry and pre-gelled sensors [11, 20]. All of these studies were done using "passive" Ag–AgCl sensors, which have changed very little since their introduction more than 50 years ago [2]. No comparative studies can be found for so-called "active" or "dry" sEMG sensors, which contain the front end of the amplification stage within close proximity to the electrode contacts. The ability of this set-up to convert the high-impedance properties of the skin to low impedance output of the amplifier makes them far less sensitive to the variable impedance of the electrode–skin interface [12]. As a result, these sensors are far less prone to capacitive coupling to noise and interference sources as the signal wire makes its way from the sensor site to the recording apparatus [2]. Active sEMG sensors were first introduced by De Luca et al. [5] and are now the de facto sensor of choice for sEMG measurement in the laboratory.

The purpose of this study is to compare the effects of different mechanical perturbations on the electro-mechanical stability of active sEMG sensors, for both wet (perspiration) and dry (non-perspiration) conditions. It focuses on factors of sensor design, as well as procedures used to interface them with the skin that may improve the likelihood of attaining high-fidelity sEMG signals under recording conditions in which there is excessive body movement or long-term activity. Although some of these factors relating to signal fidelity could have been assessed utilizing voluntarily elicited EMG signals, the extensive experimental constraints required to obtain reproducible data across subjects led us to adopt a more direct approach utilizing externally induced measures of electro-mechanical stability.

The first part of this study addresses the question of whether sensors with different detection surfaces and adhesive tapes perform differently when tested for their ability to maintain electrical contact with the skin. Adequate sensor adhesion to the skin is an important mechanical property for maintaining sEMG signal fidelity during vigorous activities because unstable contact with the skin can result in signal artifacts or complete signal detection failure [15]. The second part of this study addresses the question of whether sensors with different conductive interfaces perform differently when tested for electrical stability following shear and normal mechanical perturbations. Future studies could incorporate measures of voluntarily elicited EMG signals in addition to the externally induced measures adopted here to provide a more complete assessment of sensor design on signal fidelity.

2 Methods

2.1 Electro-mechanical tests

2.1.1 Adhesive peel test

Peel adhesion measures the force required to remove a self-adhesive tape from a standard surface at a specific angle and speed [7]. Peel tests are commonly used in industry to mechanically evaluate the adhesive properties of single- and double-sided tapes. The 90-degree Peel Test (PSTC-3), one of the more common standardized tests used in industry for measuring adhesion [7], was modified in our experiment to provide an in situ test for evaluating adhesion of a sEMG sensor to the skin. A peel test device and mounting platform were constructed for this purpose as illustrated in Fig. 1. The device uses an electric motor geared to peel the sensor from the skin at a constant velocity of 30.5 cm/min and at a 90° angle with respect to the undisturbed skin. These settings approximate the peel rate and direction of the PSTC-3 test. The device contains a load cell (Interface Model MB-50; nonlinearity = ±0.03%, hysteresis = ±0.02%) for continu-

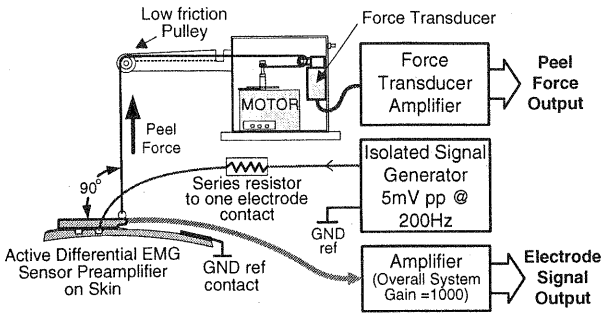

Fig. 1 The peel test device used to test adhesion of the sensors to the skin. The device uses an electric motor geared to peel the sensor from the skin. It contains a force transducer for continuously monitoring peel force applied at right angles to the sensor via a low friction cable/pulley system. The sensor contains a high-impedance differential preamplifier with each detection contact placed on the skin. An isolated signal generator delivers a 5 mV, 200 Hz sine wave to one of the detection contacts of the sensor through a 6.2-MΩ series resistor. During the peel test, the force and sensor output signals are recorded and used to characterize progressive changes in contact impedance

ously monitoring peel force applied to the sensor via a low friction cable/pulley system. A mechanical modification was made to the body of the sensors to provide a secure post at one end from which the peel test device could be attached. The sensor contained a high-impedance ($Z_{in} > 10^{15}\Omega//2$ pF) differential preamplifier with each detection contact placed on the skin. An isolated signal generator was used to deliver a 5 mV, 200 Hz sine wave to one of the detection contacts of the sensor through a 6.2-MΩ series resistor. This configuration formed a resistive divider network with the electrode contact/skin impedance acting as a shunt. Signals generated across this shunt impedance are detected at one of the differential inputs of the sensor preamplifier. An increase in signal amplitude therefore corresponds to an increase in shunt impedance. During a peel test, this amplitude is recorded and used to characterize progressive contact failure. Force transducer and sensor output signals were sampled at 1,024 Hz using a 16-bit A/D card (National Instruments) and stored on a PC for later analyses.

2.1.2 Mechanical disturbance test

The test simulates "real-world" conditions encountered when attempting to record sEMG signals during vigorous activities where limb movement and impact with external objects (such as a foot making contact with the floor) can degrade the fidelity of the signal by the presence of motion artifacts. In this study, assessment of electro-mechanical stability was measured for sEMG sensors applied to the forearm. A test device was constructed to standardize the delivery of forces to the forearm by having the subject grasp the handle of a custom-made leaf spring mounted to a support surface (Fig. 2). Normal and shear forces were applied to the sensors by positioning the leaf spring either parallel or at right angles to their orientation on the forearm, as depicted in the figure. Shear forces would thereby tend to move the sensor parallel to the skin surface, whereas normal forces would tend to move the sensor at right angles to the skin surface. Impulse perturbations were produced by asking the subject to relax their test arm while the operator displaced the leaf spring a fixed distance and then released it. This type of perturbation was selected to assess the electro-mechanical stability of the sensor when a limb is suddenly accelerated by external forces. Sinusoidal perturbations were produced by having the subject move the handle of the leaf spring in a sinusoidal trajectory. Signals from uniaxial accelerometers (DelSys, Inc.) located on the test forearm (Fig. 2) were displayed on a monitor to provide feedback for guiding the subject in producing the desired trajectory. Accelerometer data were also used to normalize the resulting signal artifacts. Subjects underwent a preliminary training period to learn to accurately produce the trajectory and accelerate the forearm smoothly within a range of ±2 G at a frequency of 4–5 Hz. Signals from the sensors during the 15 sinusoidal perturbations in shear and normal directions, respectively, were recorded at a gain of 1,000 using a custom amplifier, band passed at DC-450 Hz, sampled at 1,024 Hz, and stored using a 16-bit A/D card. Examples of sinusoidal and impulse trajectories are shown in Fig. 2. The signal artifacts resulting from the normal and shear components of the sinusoidal perturbations were measured in μV pp with respect to the input, band passed at 1–20 Hz, normalized with respect to either normal or shear components of the peak-to-peak accelerations, and averaged for five repetitions of the sinusoidal trajectory. The same processing was done for calculating the signal artifacts from the impulse perturbations, except that these signals were band passed at 1–50 Hz.

2.2 Sweat protocol

The Sweat protocol was devised to evaluate the electro-mechanical performance of the sensors in the presence of perspiration on the skin. Accumulation of perspiration on the forearm was accomplished by progressively raising the subject's body core temperature by having them pedal a cycle ergometer. Localization of perspiration to the forearm was achieved by

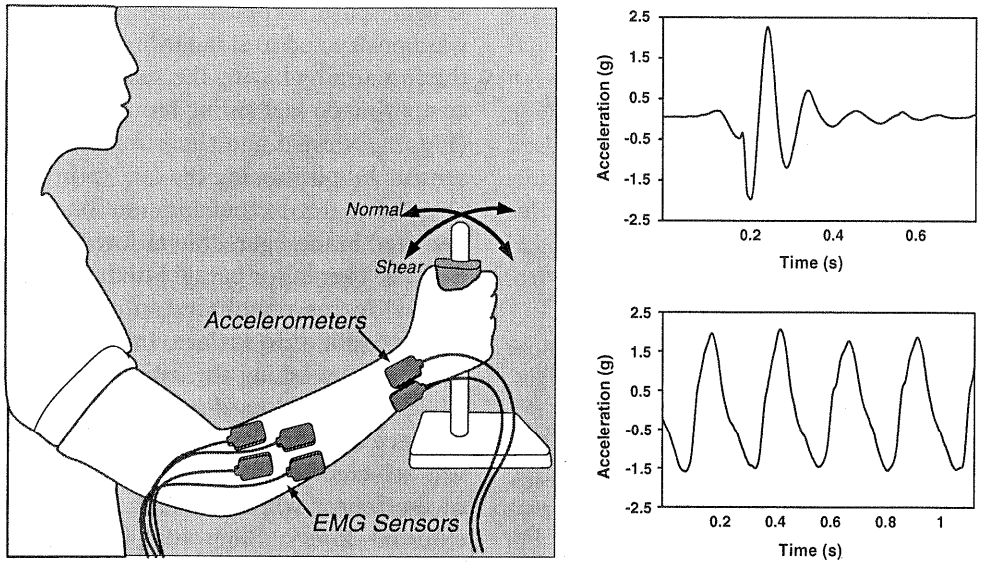

Fig. 2 A drawing of the experimental set-up used to implement the Mechanical Disturbance test. A subject with four sEMG sensors and two accelerometers (DelSys, Inc.) on the forearm is shown holding the handle of a leaf spring device. The handle is oriented either in line with, or at right angles to, the orientation of the sensors. Normal accelerations are produced by internal and external rotations of the shoulder. Shear accelerations are produced by flexion and extension of the shoulder. Sinusoidal perturbations are produced by asking the subject to actively move the handle with the aid of visual feedback (not shown). Impulse perturbations are produced by the investigator deflecting and immediately releasing the handle. Examples of accelerometer data plots for impact (*upper right*) and sinusoidal (*lower right*) perturbations are illustrated

having the subject's forearm in a sealed "sweat chamber" to limit evaporation. The choice of a cycle ergometer was based on its effectiveness in achieving an exercise intensity that progressively raises body core temperature without causing excessive movement of the forearm where the sensors are located. The sweat chamber was constructed of clear Plexiglas® to provide visibility of the forearm and sensors. The entry panel for the arm was fitted with a rubber seal to maintain chamber temperature and humidity while the arm is in place. Sliding panels on the top of the chamber allowed the operator to access the sensors without removing the test arm from the chamber. Chamber and forearm skin temperature, and chamber relative humidity, were monitored at baseline and throughout the Sweat protocol. Ambient room temperature was maintained at 70°F/21°C.

The intensity of the cycle ergometer exercise protocol was specified based on pilot tests in five subjects to characterize the relationship between cycle workload (as determined by pedaling frequency, resistance, and duration) and the accumulation of perspiration on the forearm. Accumulation of perspiration was measured quantitatively by weighing paper blotters applied to the skin of the forearm at various time intervals into the cycle exercise. Based on these preliminary tests, a 150 W workload for 14 min duration was specified for the Sweat protocol. This workload proved adequate to produce significant accumulation of perspiration on the forearm while being well tolerated by a non-athletic subject population.

2.3 Experimental procedure

Twenty-four subjects (12 males; 12 females; mean age = 24.1 ± 3.9 years; mean weight = 64.4 ± 13.4 kg) volunteered for part 1 of the study and five subjects (4 males; 1 female; mean age = 23.1 ± 3.3 years; mean weight = 64.0 ± 8.8 kg), volunteered for part 2 of the study. Subjects were screened for cardiovascular and musculoskeletal conditions which could be aggravated by their use of the bicycle ergometer in the Sweat protocol. Subjects were excluded if the skin on their forearm was damaged from cuts or open sores. All subjects read and signed an informed consent form according to procedures set forth by an Institutional Review Board.

Prior to each experiment, the skin was prepared to remove body oils and dried flaky skin from the test forearm prior to placement of the sensors. The procedure consisted of shaving body hair on the forearm with a disposable razor and wiping the area several times with an alcohol prep pad. The outermost layer of the skin was then debrided following a method described by de Talhouet and Webster [5] in which successive outer layers of dead skin were removed through

repeated application and peeling of hypoallergenic skin tape (3 M Micropore®).

2.3.1 Part 1

The effects of sensor surface contour and type of adhesive used to maintain contact between the sensor and the skin were assessed for peel adhesion before and after the Sweat protocol. Three active sEMG sensors (Series DE-2.1, DelSys, Inc.) with the following specifications: $G = 10$, $Z_{in} > 10^{15}\Omega//2$ pF, noise = 1.2 uV RMS, mass = 3 g, electrode contact material 99.9% Ag were tested concurrently and compared (Fig. 3a). The first two sensors (Flat/Adhesive 1 and Flat/Adhesive 2, respectively) were tested in conjunction with different double-sided adhesive tapes, as outlined in Table 1. One of the sensors (Adhesive 1) was tested with an adhesive tape rated at 2.0 force lb./in (180° peel adhesion; PSTC-1 test method) and the other (Adhesive 2) was tested with an adhesive tape rated at 3.7 force lb./in (180° peel adhesion; PSTC-1 test method). The skin-side of the encapsulation of these two sensors was non-contoured ("Flat"). The third test sensor (Contour/Adhesive 2) was developed as a prototype modification to the DE-2.1 sensor by contouring the encapsulation adjacent to its detection bars (Fig. 4) to improve adhesion of the sensor to the skin. It was configured for testing with the more adherent Adhesive 2 tape.

The adhesive tapes used to secure the sensors to the skin were made from commercially-available double-sided medical grade tapes (Avery Dennison™, Pasadena, CA, USA) that were cut to the same dimensions for all three test samples and had openings provided to allow the two detection bars to protrude through the tape and liner. The shelf life of the tapes used in these experiments was within the recommended range specified by the manufacturer and all utilized the same protective silicone liners which were peeled away immediately before securing the tape to the sensor and skin. A summary of the physical dimensions of the sensors, their detection surfaces, and double-sided adhesive tape is provided in Table 1.

Two samples of each of the test sensors were arranged on the forearm so that peel force data could be collected at baseline and again at 14 min immediately following the Sweat protocol. Sensors were arranged in two adjacent parallel rows (i.e. one row for each set of samples) using a template which defined the relative location of the six sensors with respect to each other. The template was oriented according to a line drawn between the middle digit and the prominence of the lateral epicondyle of the elbow. The three different sensors were arranged on the template using a random placement scheme. Sensors were allowed to "settle" for 5 min to allow a fixed time period for the adhesive

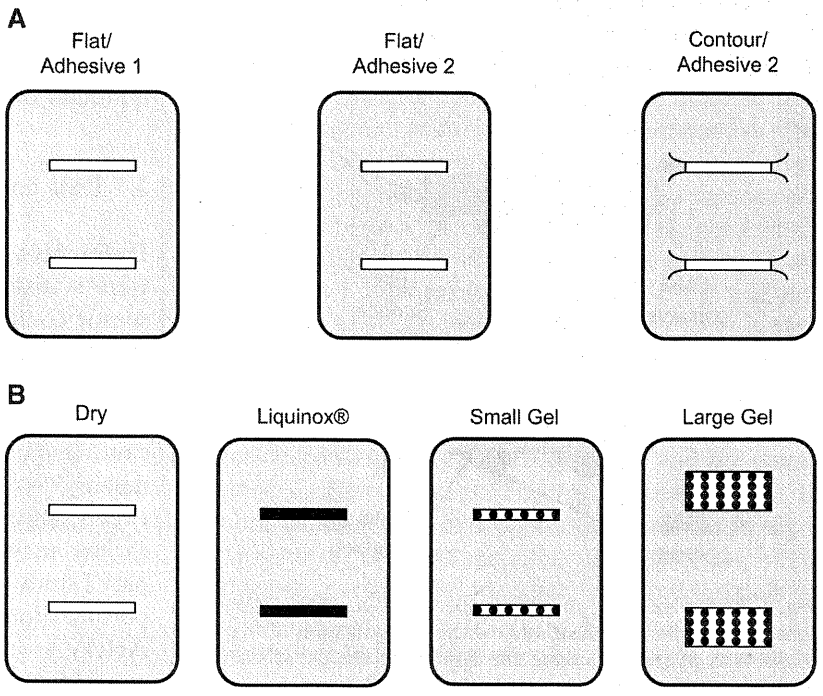

Fig. 3 Illustration of the different sEMG sensor configurations tested in the study. The *upper panel* **a** identifies the three test samples evaluated for differences in adhesion in the part 1 study, and the *lower panel* **b** identifies the four test samples evaluated for motion artifact in the part 2 study. Note that all dimensions of the adhesive are identical and 3 cm × 3 cm

Table 1 Dimensions and other physical characteristics of the sensors tested in the part 1 and part 2 studies

Sensor	*L* (mm)	*W* (mm)	*S* (mm)	BL (mm)	BW (mm)	Tape adhesion[a] (force lb/in)	Tape area (mm^2)	Conductive interface
Part 1: Peel adhesion study								
Flat/Adh1	30	20	10	10	1	2.0	600	None
Flat/Adh2	30	20	10	10	1	3.7	600	None
Contour/Adh2	30	20	10	10	1	3.7	600	None
Part 2: Mechanical perturbation study								
Dry	30	20	10	10	1	3.7	600	None
Liquinox	30	20	10	10	1	3.7	600	Liquinox®
Small Gel	30	20	10	10	1	3.7	600	Gel (small)
Large Gel	30	20	20	12.5	5.0	3.7	600	Gel (large)

L Sensor length, *W* sensor width, *S* separation between detection surfaces, *BL* detection surface length, *BW* detection surface width

[a] Liner adhesion values provided by the manufacturer and specified per inch width of tape for 90° Peel adhesion (PSTC-1) tests

to be in contact with the skin. A randomized procedure was also used to select the order in which the sensors were peeled.

2.3.2 *Part 2*

The effects of different skin preparations and conductive hydrophilic gels on motion artifact resulting from the Mechanical Disturbance tests were assessed before and again after the Sweat protocol. Three of the four test samples shown in Fig. 3b [i.e. Dry (no conductants), Liqui-Nox® (a surfactant), and Small Gel (narrow strips of hydrophilic gel)] were tested using the same commercially available flat surface EMG sensors as in the part 1 study. The fourth test sample (Large Gel) was tested using a sensor similar to the other test samples except that the size and separations of the detection bars were enlarged to provide a greater surface area for the application of a wider strip of hydrophilic gel. The gel preparations were made using a 2 mm thick conductive-adhesive gel matrix (3 M™, St. Paul, MN, USA) that was cut to the size of the respective detection surfaces of the sensors. All of the sensors utilized the same Adhesive 2 tape to secure them to the forearm (Table 1).

As described in the part 1 study, sensors were arranged according to pre-designated sites that were specified using a template on the forearm (Fig. 2). Similarly, a 5 min "settling" period was provided between the time of adhering the sensor to the skin and conducting the baseline test. A randomized procedure was used to select the order in which the sensors were tested, as well as the order in which the four different mechanical disturbance perturbations were carried out. Signal artifacts resulting from the normal and shear components of the sinusoidal perturbations were acquired at Baseline and at 14 min of the Sweat protocol.

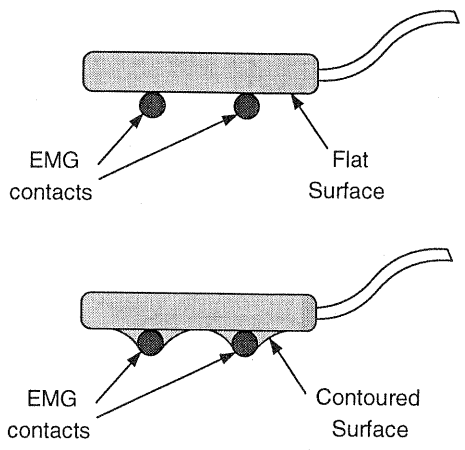

Fig. 4 Profile views of the flat (*upper*) and contoured (*lower*) sensors are shown to illustrate how the encapsulation of the flat sensor was altered to create the contoured sensor which was tested for peel adhesion in part 1 of the study

2.4 Data analysis

Differences in mean peel forces for the part 1 study were statistically evaluated using an ANOVA where sensor configuration was defined as a grouping factor and trials conducted before and after the Sweat protocol were defined as a repeated measure. In those instances where main effects were statistically significant, planned pair-wise comparisons between group means were computed to compare performance between individual sensor configurations. A similar statistical analysis was done for the artifact data in the part 2 study where the results of each of the mechanical perturbation tests were evaluated separately using the ANOVA statistic. Statistical significance was set at $p < 0.05$ for all of the analyses.

3 Results

3.1 Part 1

Relative humidity within the chamber increased from 28 ± 3% at baseline to 82 ± 11% half-way into the 14-min cycling period, and to 99 ± 0.2% by the end of the cycling period. Mid-way into the Sweat protocol moisture could be seen in the chamber and on the forearm. By the end of the cycling period, there was noticeable condensation on the walls of the chamber, and the forearm was drenched with perspiration. Skin and chamber temperature also increased during, and following the Sweat protocol as indicated in Fig. 5.

Two types of peel force responses were observed: (1) a gradual loss of electrode contact with the skin occurring at a low peel force as indicated by slowly increasing signal amplitude (Fig. 6, left panel), and (2) a rapid loss of electrode contact with the skin occurring at a high peel force as indicated by an abrupt increase in signal amplitude (Fig. 6, right panel). The peel responses can be divided into three phases. The first phase is the quiescent adhesion period representing the signal shunted by the impedance of the electrode/skin contact. The amplitude is in the range 20–100 μVpp depending on skin conditions. The second phase is the period of force-dependant increase in electrode/skin impedance during the process of peeling the sensor from the skin. It includes the sequence of events leading up to and including contact failure of both electrode bars. The third phase is the period when both inputs to the sensor are floating. The amplitude of the signals during this period is no longer representative of the impedance conditions and is therefore not incorporated in the analysis. Note in the lower panels that the force corresponding to the onset of the gradual rise in skin impedance occurs at a lower peel force in the left panel compared to the more abrupt changes in the right panel. In all instances, the sensor was physically removed from its location on the forearm as a result of a loss of adhesion between the skin and the tape rather than loss of adhesion between the sensor encapsulation and the tape.

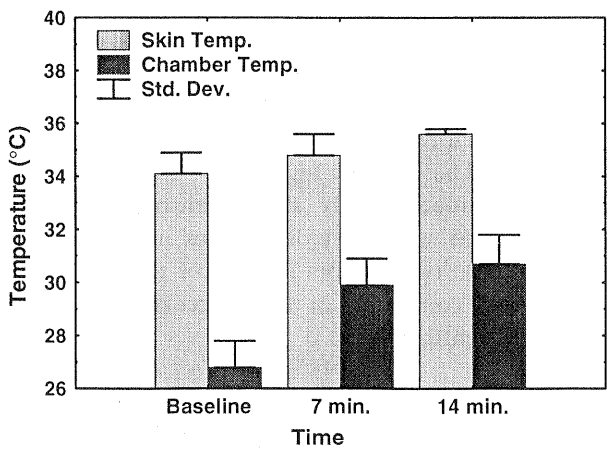

Fig. 5 Skin temperature and sweat chamber temperature (mean ± SD) during the part 1 study. Data are presented for Baseline, 7, and 14 min of cycling during the Sweat protocol

Peel test results are summarized in Fig. 7, where mean peel force data were significantly different between the three test sensors [$F(2,63) = 28.14$; $p < 0.0001$]. As shown in the figure, significant differences in mean peel force were present when statistical comparisons were carried out separately for each trial before and after the Sweat protocol, respectively. The use of the more adherent double-sided tape (Adhesive 2) on the flat sensor resulted in an average increase in peel force of 99.5%. Contouring the detection surface encapsulation of the flat sensor resulted in an increase in mean peel force of 82.9% when tested using the Adhesive 2 tape. Although some individual test samples lost as much as 65% of their peel force when tested following the Sweat protocol, overall the differences before and after the Sweat protocol were highly variable and failed to reach a level of significance [$F(1,63) = 4.14$; $p = 0.40$].

3.2 Part 2

Relative humidity within the chamber increased from a mean of 27 ± 2.2% at baseline to a mean of 99 ± 0.2% by the end of the Sweat protocol. These increases were consistent with those of the part 1 study.

Differences in artifact production due to the type of sensor studied, the timing of the tests relative to the Sweat protocol, and the possibility of interactive effects between these factors were all significant following an ANOVA analysis, which were computed separately for each of the four mechanical perturbation conditions. The presence of significant interactive effects between *Sensor* and *Trial* factors demonstrates that individual differences in artifact production for the different sensors depended in large part on whether baseline data or data collected after the Sweat protocol were analyzed. Planned statistical comparisons were therefore used to analyze such differences and are summarized in Figs. 8 and 9. The figures demonstrate that both sensors with hydrophilic gel resulted in significantly more artifact than either the Dry or Liqui-Nox® sensors, particularly for data acquired immediately following the Sweat protocol. The reduction in electromechanical stability associated with the hydrophilic gel sensors tested following the Sweat protocol was

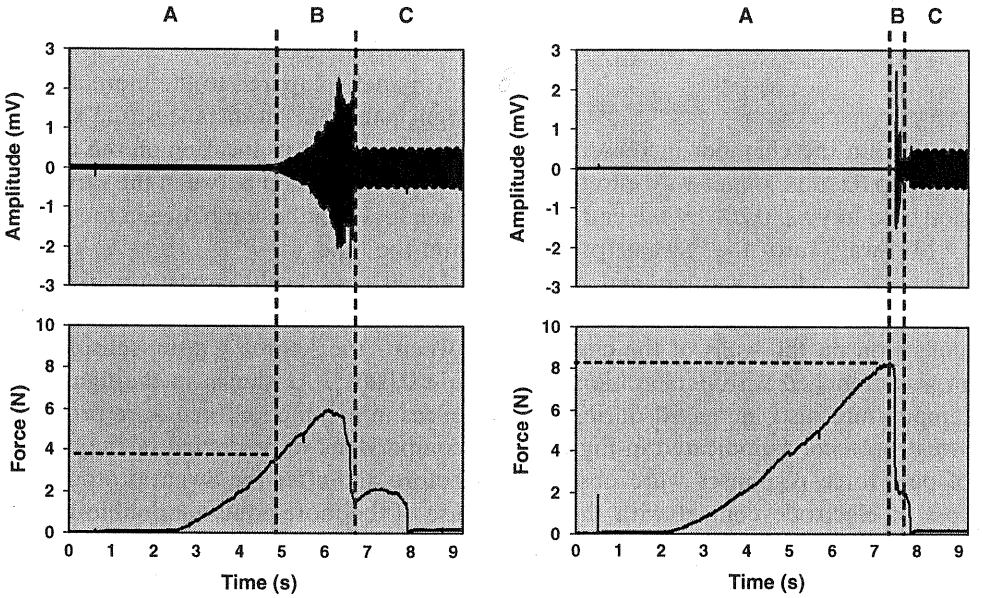

Fig. 6 Examples of two types of adhesion failure during a peel test are plotted for relatively slow (*left panel*) and relatively fast (*right panel*) loss of adhesion. The plots have been divided into three phases. The first phase "A" is the quiescent adhesion period representing the signal shunted by the impedance of the electrode/skin contact. The amplitude is in the range 20–100 μVpp depending on skin conditions. Phase "B" indicates the period of force-dependant increase in electrode/skin impedance during the process of peeling the sensor from the skin showing the sequence of events leading up to and including contact failure of both electrode bars. Phase "C" represents the period when both differential inputs to the sensor are floating. The amplitude of the signal during this period is no longer representative of the impedance conditions and therefore not incorporated in the analysis

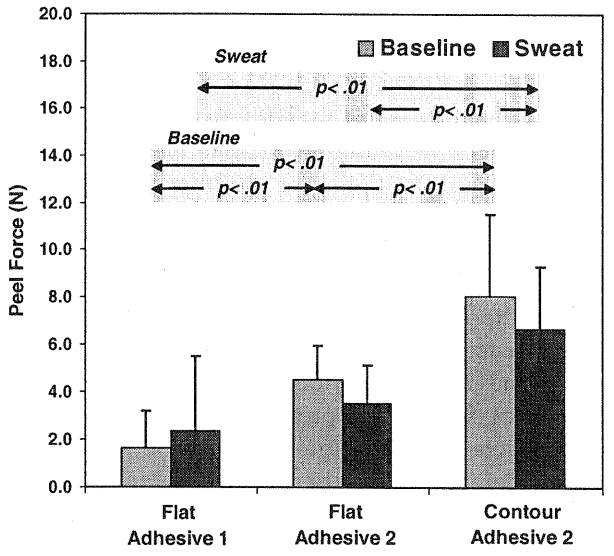

Fig. 7 Comparison of peel test results (mean ± SD) for Flat/Adhesive 1, Flat/Adhesive 2, and Contour/Adhesive 2 sensors, respectively, which were evaluated in part 1 of the study. Peel forces are shown for trials conducted at Baseline and again following 14-min of cycling for the Sweat protocol. Statistically significant differences between mean peel force values for each of the trial periods and sensors are indicated by the *arrows* in the *shaded area*

significant for all of the mechanical perturbation conditions. In contrast, only the Large Gel sensor had significantly greater artifact when compared to the other sensors for tests conducted prior to the Sweat protocol and only as a result of normal and shear impact perturbations (Fig. 9a, b, respectively). These two perturbation conditions were the most effective in significantly reducing the electromechanical stability of the hydrophilic gel sensors, and the resulting artifact production was increased according to the amount of gel present; i.e. the Large Gel sensor had significantly more artifacts than the Small Gel sensors for trials conducted before as well as after the Sweat protocol (Fig. 9a, b). The Dry and Liqui-Nox® sensors were the most electromechanically stable sensors tested and there were no significant differences in performance between these two sensors for any of the mechanical perturbation conditions or trials occurring before or after the Sweat protocol.

4 Discussion

The findings of this study demonstrate that: (a) relatively simple design changes made to the external

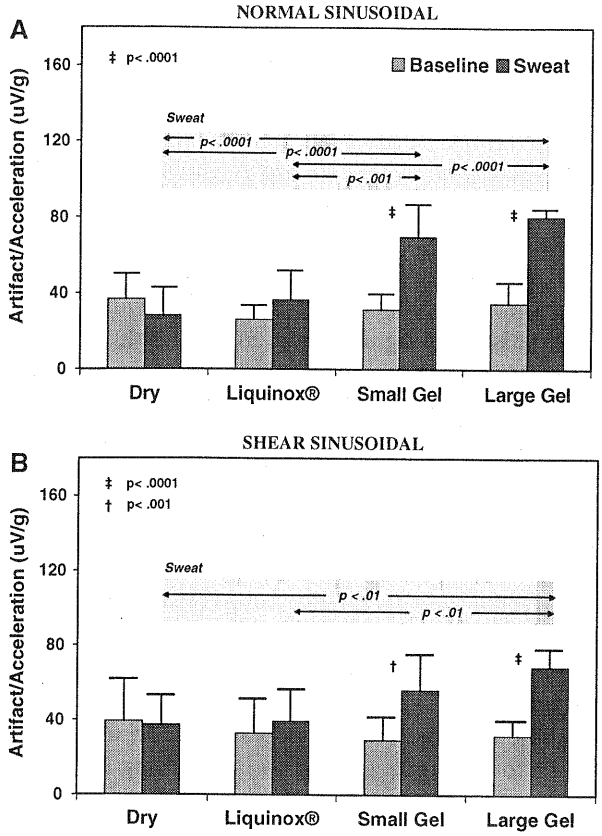

Fig. 8 Comparison of mechanical perturbation test results (mean ± SD) for normal (**a**) and shear (**b**) sinusoidal disturbances from part 2 of the study. The artifact data was normalized with respect to the amplitude of acceleration of the forearm. Data are plotted separately for the four sensor preparations (Dry, Liqui-Nox®, Small Gel, and Large Gel) which were compared for baseline measurements and measurements following the Sweat protocol. Significant findings from a repeated-measures ANOVA are shown for planned comparisons between sensors (*arrows* in the *shaded areas*) and between trials (*symbols*)

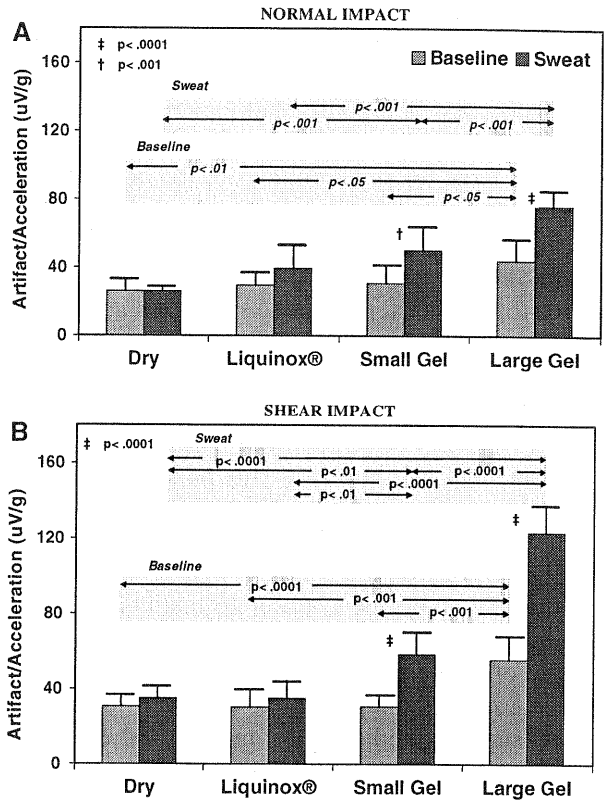

Fig. 9 Comparison of mechanical perturbation test results (mean ± SD) for normal (**a**) and shear (**b**) impact disturbances from part 2 of the study. The artifact data was normalized with respect to the amplitude of acceleration of the forearm. Data are plotted separately for the four sensor preparations (Dry, Liqui-Nox®, Small Gel, and Large Gel) which were compared for baseline measurements and measurements following the Sweat protocol. Significant findings from a repeated-measures ANOVA are shown for planned comparisons between sensors (*arrows* in the *shaded areas*) and between trials (*symbols*)

surface of the sensor, and the adhesive properties of the tape used to secure it to the skin, can significantly improve the electrical contact between the sensor and the skin; and (b) the application of conductive hydrophilic gels between the sensor detection surfaces and the skin can lead to significant increases in signal artifact when the sensor is exposed to mechanical perturbations, particularly when the skin is wet as a result of perspiration.

The first part of this study demonstrated that adhesion of the sensor to the skin, as measured by peel force, was significantly improved by changing the double-sided tape and external contour of the sensor. The Flat/Adhesive 1 sensor, which did not incorporate either of these modifications, had the lowest peel force values. Replacing the double-sided tape to one with a more adherent adhesive (Flat/Adhesive 2) resulted in significant improvements in peel adhesion which was substantially enhanced by adding contours to the flat surface (Contour/Adhesive 2). This progressive, and more than fourfold increase in peel adhesion, was present for trials conducted before and following the Sweat protocol.

The two sensor modifications studied were specifically selected for their potential to improve adhesion without modifying the footprint of the sensor or the amount of tape used to secure it. The sensor and tape footprint are important design considerations when developing a sensor. The DelSys Inc. sEMG sensor utilized in these experiments has a footprint that was developed as a compromise to allow EMG signals to be detected from relatively small superficial muscles of the body (such as found in the face, hands and forearms) as well as relatively large muscles of the body

(such as in the thigh or torso). Increasing the sensor footprint to increase the surface area of double-sided tape in contact with the skin must be weighed against the possible loss in usability that may result if the tape interferes with adjacent sensors or when sensors become too large for small muscles of the body or when recording from toddlers and children. Larger sensors may also have an inherent disadvantage when studying dynamic activities, due to the added mass and resultant inertial forces transferred to the skin, leading to motion artifacts. This study examined the effects of increasing the sensor footprint to increase the adhesive surface area and accommodate larger and more widely spaced electrodes. Such modifications may improve the detection area [2]; however, this advantage must be weighed against the undesirable effect of increasing signal cross-talk from neighboring muscles [4]. One of the implications of this study is that it is possible to improve the ability of a sensor to maintain electrical contact with the skin without resorting to increases in the size of the sensor footprint and the corresponding surface area of the tape used to adhere it to the skin.

The surface modifications made to the Contour sensor in the part 1 study consisted of rounding the skin-side of the sensor to equalize skin tension in the detection bar area; thereby reducing peel stresses. Providing a smooth surface for the adhesive tape in the areas where the encapsulation meets the detection bars should theoretically minimizes the tendency of the bars to push the sensor away from the skin at these locations. The contouring of the encapsulation was designed to eliminate possible gaps between the side of the electrode bars and the skin where moisture may pool and eventually disrupt adhesion of the sensor to the skin (visual observation of the flat sensors following the Sweat protocol confirmed that perspiration and moisture was pooling in this gap). However, the fact that mean peel forces decreased by approximately the same amount for the contoured and non-contoured sensors following the Sweat protocol indicates that contouring did not provide a significant advantage when perspiration was present. The relatively high standard deviations in Fig. 7 are an indication that the peel test results varied considerably across individual subjects. Such individual differences could not be accounted for by the relatively small variance in % humidity of the sweat chamber.

The presence of two types of peel force failure (i.e. "slow" vs. "fast" failure) depicted in Fig. 6 may also have practical consequences when these sensors are exposed to "real-world" perturbations. Sensors that lose contact with the skin, but take relatively longer to dislodge from the body, may not be immediately recognized as a problem by the user who typically relies on visual inspection of the sensor to ascertain that the contact between the sensor and the skin is maintained. In practice it is preferable to have a catastrophic failure rather than a failure that creeps.

The most noteworthy finding of the part 2 study was that the use of a hydrophilic gel, which is commonly considered to be an effective method of improving biosignal quality, was associated with greater motion artifact when mechanically perturbed. Such findings were statistically significant even among the relatively small subject population tested. It was beyond the scope of this work to investigate the source of these artifacts. However, because this effect was most pronounced for shear impact perturbations as well as for perturbations following the Sweat protocol, it is likely that the viscoelastic and hydrophilic properties of the gel were a dominant contributing factor in producing the movement artifact. Gel can be considered as a fluid material with an upper and lower surface parallel to the skin surface. Because the lower surface is adhered or fixed to the skin surface, the upper surface and its attachment to the sensor body are free to move in response to the force applied to it, resulting in a deformation of the gel substance. The amount of deformation per unit height of the material is referred to as the shear strain and is proportional to the viscosity of the material. Under the test conditions, the gel is likely to become less viscous due to increases in body temperature and absorption of water by the gel from the skin and accumulated perspiration. The resulting increase in deformation of the gel in response to the mechanical perturbations (particularly shear perturbations) would cause the sensor to move with respect to the skin resulting in motion artifact. The more gel between the sensor and the skin, the more pronounced the effect, which is what we observed when artifacts for the Small Gel and Large Gel sensors were compared. In contrast, the Dry and Liqui-Nox® sensors did not have viscoelastic materials applied to their detection surfaces and accordingly had significantly less motion artifact.

These findings contradict the common perception that gel improves the signal quality of biosensors. This perception is based primarily on ECG and EEG studies in which passive sensors with receptacles for containing the gel were studied rather than active sEMG sensors [8, 10, 13, 19]. Gels readily conform to the body surface and separate the metal electrode from making direct contact with the skin, thereby stabilizing the electrode-electrolyte interface [10] and reducing baseline noise [8, 23] and motion artifacts [19]. However, not all noise sources can be attributed to the

electrode–electrolyte interface. Potentials that develop across the outer dermal layer and the electrolyte are also problematic [8, 16]. The gel–skin interface has been studied separately from the electrode–electrolyte interface and found to be significantly influenced by the type of skin preparation and gel used, as well as the location of the sensor on the body [8, 13].

Deformation of the skin by the displacement of the sensor will change the potentials emanating from the gel–skin interface, as well as the more stable metal–electrolyte interface associated with the gel, giving rise to motion artifacts [10]. The significant increase in motion artifact observed for the sensors tested with hydrophilic gel in our study were likely due to the effects of skin deformation that resulted from the movement of these sensors in response to the mechanical perturbation. Active sEMG sensors typically have a greater mass than disposable-gel or receptacle-style ECG sensors, and the larger momentum would likely produce more skin deformation. Future development of active sEMG sensors will need to find ways of reducing their mass to minimize this source of movement artifact.

We limited this study to testing active sEMG sensors because of their widespread popularity in the laboratory and the lack of comparative studies in the literature. Although these sensors have a reduced need for skin preparation, conductants and skin preparations are commonly used in practice because they can facilitate ionic currents between the sensor and the skin, especially when recordings are made on individuals with dry skin. The current study suggests that the application of a conductive hydrophilic gel for this purpose should be done sparingly for recordings where mechanical perturbations normally encountered during movement may be present or where environmental conditions favor the accumulation of perspiration on the skin.

Acknowledgments The project was funded in part by SBIR awards from NASA (Contract # NAS 9-98035). We appreciate the assistance of Mr. Per Bergman in writing the data analysis software for the study and providing helpful suggestions during the planning stages of the research design and the preparation of this manuscript.

References

1. Aronson S, Geddes LA (1985) Electrode potential stability. IEEE Trans Biomed Eng 32:987–988
2. Basmajian J, De Luca CJ (1985) Muscles alive: their function revealed by electromyography, 5th edn. Williams and Wilkins, Baltimore, p 22
3. Blok J, van Asselt S, van Dijk J, Stegeman D (1997) On an optimal pasteless electrode to skin interface in surface EMG. In: Hermens HJ, Freriks B (eds) SENIAM 5: the state of the art on sensors and sensor placement procedures for surface electromyography: a proposal for sensor placement procedures. Roessingh Research and Development, Enschede, pp 71–76
4. De Luca CJ (1997) The use of surface electromyography in biomechanics. J Appl Biomech 13:135–163
5. De Luca C, Le Fever R, Stulen F (1979) Pasteless electrode for clinical use. Med Biol Eng Comput 17:387–390
6. de Talhouet H, Webster JG (1996) The origin of skin-stretch-caused motion artifacts under electrodes. Physiol Meas 17:81–93
7. DeVries KL, Borgmeier PR (2003) Testing of Adhesives. In: Pizzi A, Mittal KL (eds) Handbook of Adhesive Technology, Marcell Dekker, New York, pp. 223–253.
8. Fernandez M, Pallas-Areny R (2000) Ag–AgCl electrode noise in high-resolution ECG measurements. Biomed Instrum Technol 34:125–130
9. Gatzke RD (1974) The electrode: a measurement system viewpoint. In: Miller HA, Harrison DC (eds) Biomedical electrode technology. Academic, New York, pp 99–116
10. Geddes LA, Baker LE (1989) Principles of applied biomedical instrumentation, Chap. 9: electrodes. Wiley, New York, pp 315–452
11. Gondran C, Siebert E, Yacoub S, Novakov E (1996) Noise of surface bio-potential electrodes based on NASICON ceramic and Ag–AgCl. Med Biol Eng Comput 34:460–466
12. Hagemann B, Luhede G, Luczak H (1985) Improved "active" electrodes for recording bioelectric signals in work physiology. Eur J Appl Physiol Occup Physiol 54:95–98
13. Huigen E, Peper A, Grimbergen CA (2002) Investigation into the origin of the noise of surface electrodes. Med Biol Eng Comput 40:332–338
14. Inman VT (1953) The pattern of muscular activity in the lower extremity during walking. Calif Univ Techn Rep Ser III 25, pp 1–41
15. Kumar S (1996) Electromyography in ergonomics, In: Kumar S, Mital A (eds) Electromyography in ergonomics. Taylor & Francis, Bristol, pp 1–50
16. Merletti R, Hermens H (2004) Detection and conditioning of the surface EMG signal. In: Merletti R, Parker P (eds) Electromyography: physiology, engineering, and noninvasive applications. Wiley, New York, pp 107–132
17. Odman S, Oberg PA (1982) Movement-induced potentials in surface electrodes. Med Biol Eng Comput 20:159–166
18. Piper H (1907) Uber den willkurlichen muskeltetanus. Pflugers Arch Ges Physiol Mensch Tiere 119:301-338.
19. Roman J, Lamb L (1962) Electrocardiography in flight. Aerosp Med 33:527–544
20. Tassinary LG, Green TR, Cacioppo JT, Edelberg R (1990) Issues in biometrics: offset potentials and the electrical stability of Ag/AgCl electrodes. Psychophysiology 27:236–242
21 Tam HW, Webster JG (1977) Minimizing electrode motion artifact by skin abrasion. IEEE Trans Biomed Eng 24(2):134-139
22. Turker KS (1993) Electromyography: some methodological problems and issues. Phys Ther 73:698–710
23. Zipp P, Hennemann K, Grunwald R, Rohmert W (1980) Bioelectrode jellies for long-term monitoring. Eur J Appl Physiol Occup Physiol 45:131–145